Supplement of Atmos. Chem. Phys., 25, 17933–17951, 2025
https://doi.org/10.5194/acp-25-17933-2025-supplement

Atmospheric Chemistry and Physics
Open Access
EGU

Supplement of

Drone-based vertical profiling of particulate matter size distribution and carbonaceous aerosols: urban vs. rural environment

Kajal Julaha et al.

Correspondence to: Kajal Julaha (julaha@icpf.cas.cz) and Naděžda Zíková (zikova@icpf.cas.cz)

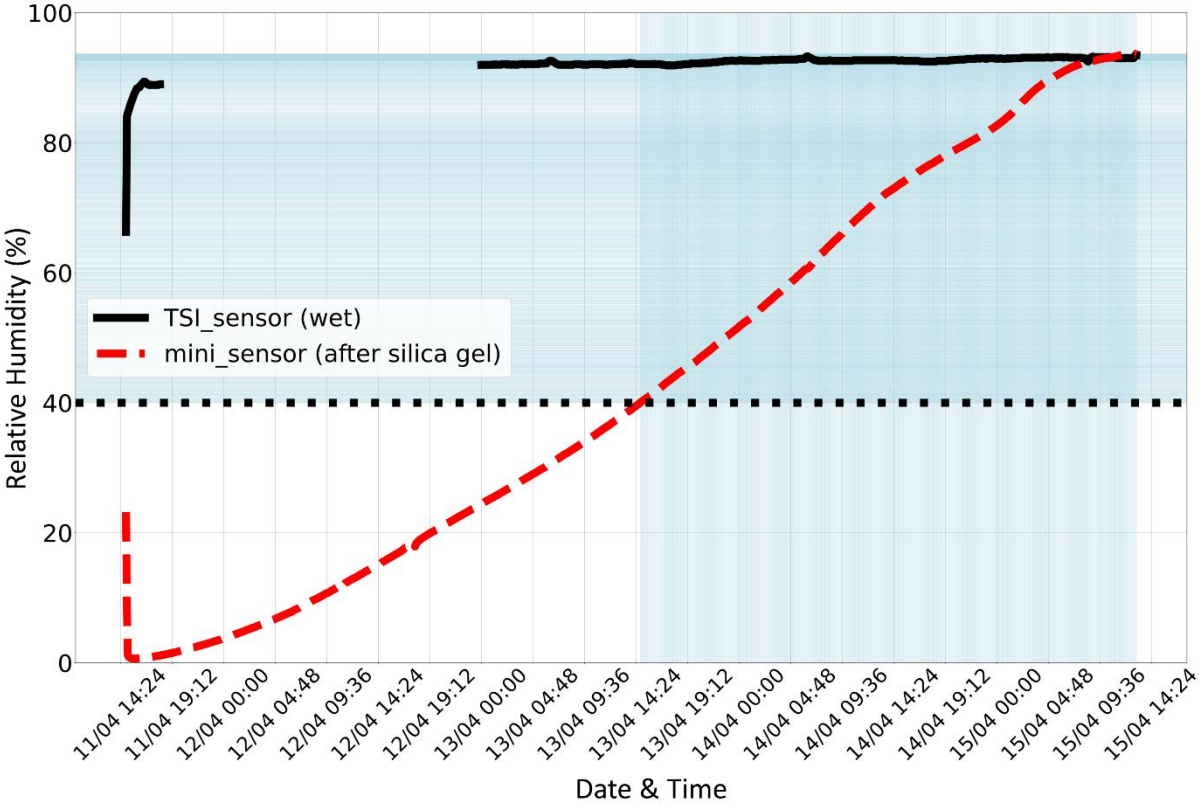

Figure S1. Variation of Relative Humidity after subjecting Air stream Dryer to 100 % RH.

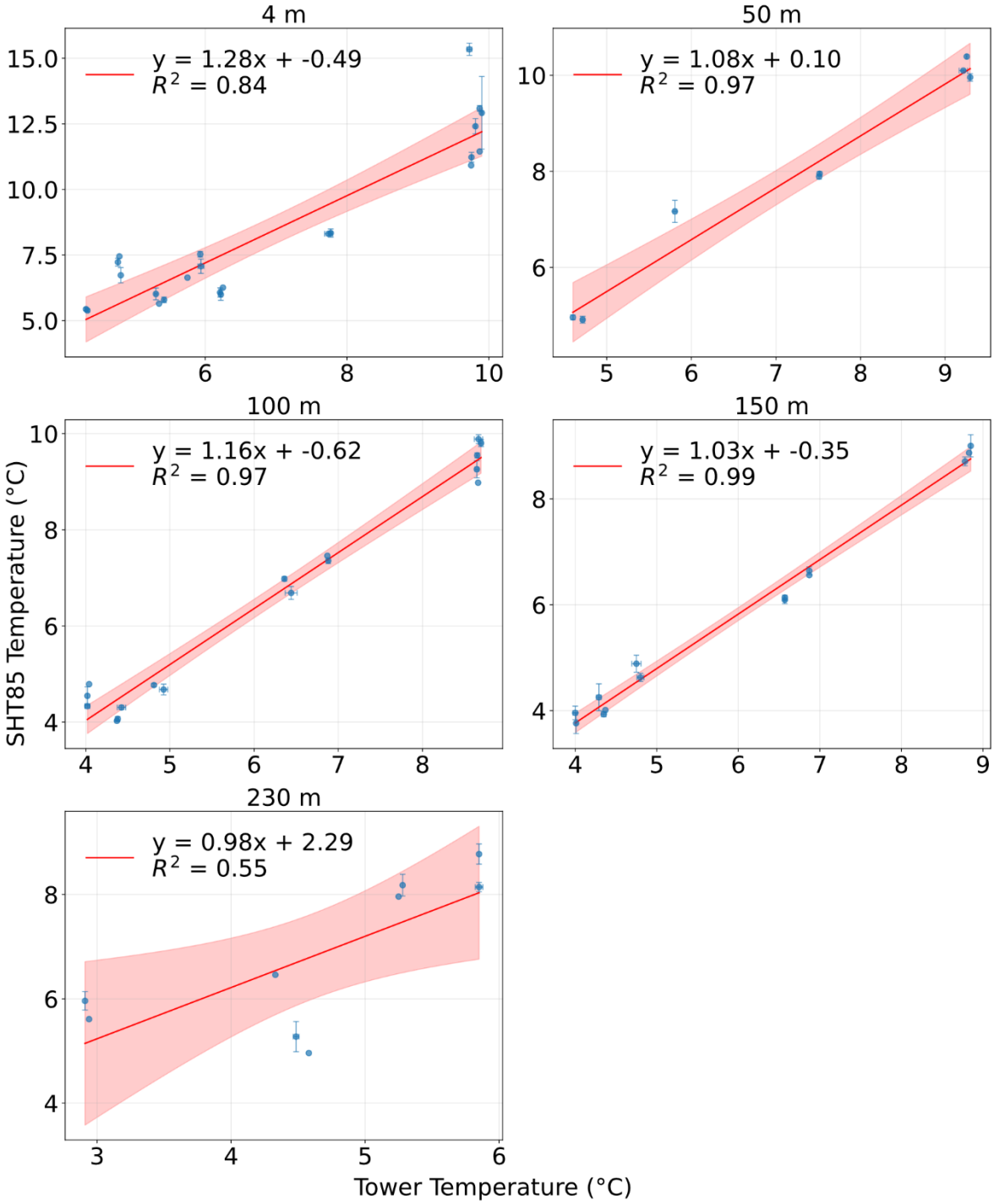

Figure S2. Correlation plot between temperature measurements obtained from the sensor SHT85 placed on the drone with OPC and from the sensors on the tower at various heights.

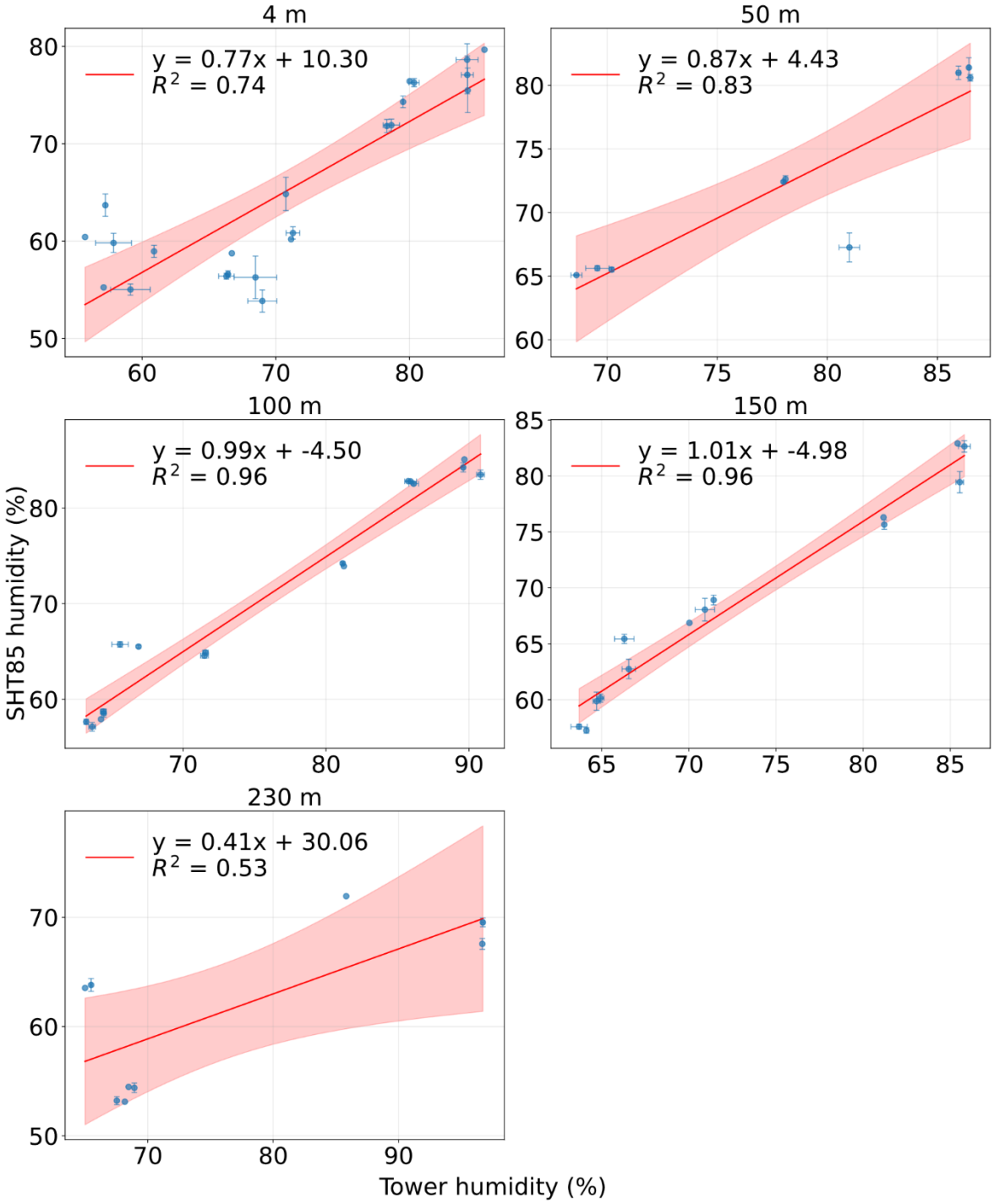

Figure S3. Correlation plot between relative humidity measurements obtained from the sensor SHT85 placed on the drone with OPC and from the sensors on the tower at various heights.

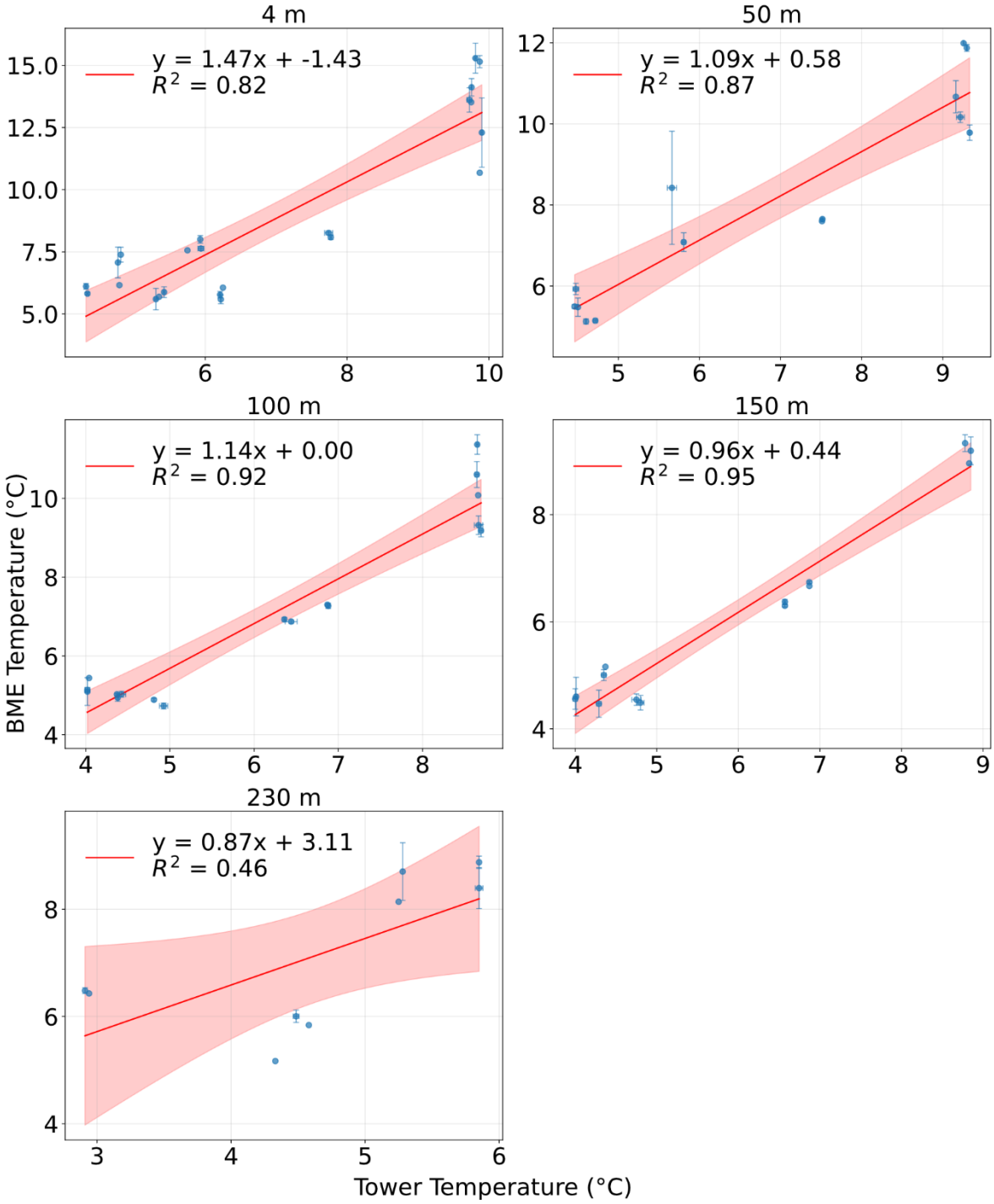

Figure S4. Correlation plot between temperature measurements obtained from the sensor BME placed on the drone with OPC and from the sensors on the tower at various heights.

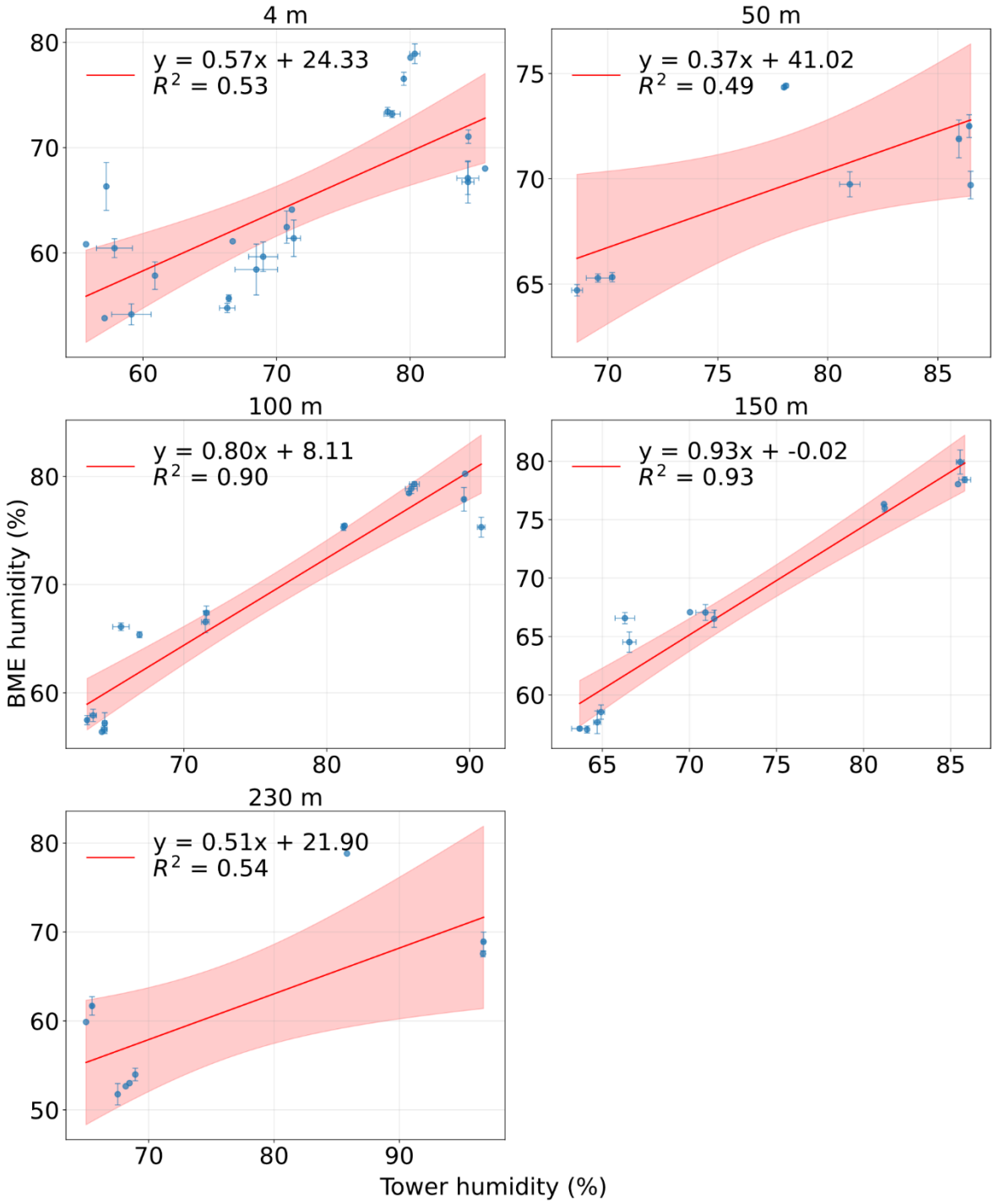

Figure S5. Correlation plot between relative humidity measurements obtained from the sensor BME placed on the drone with OPC and from the sensors on the tower at various heights.

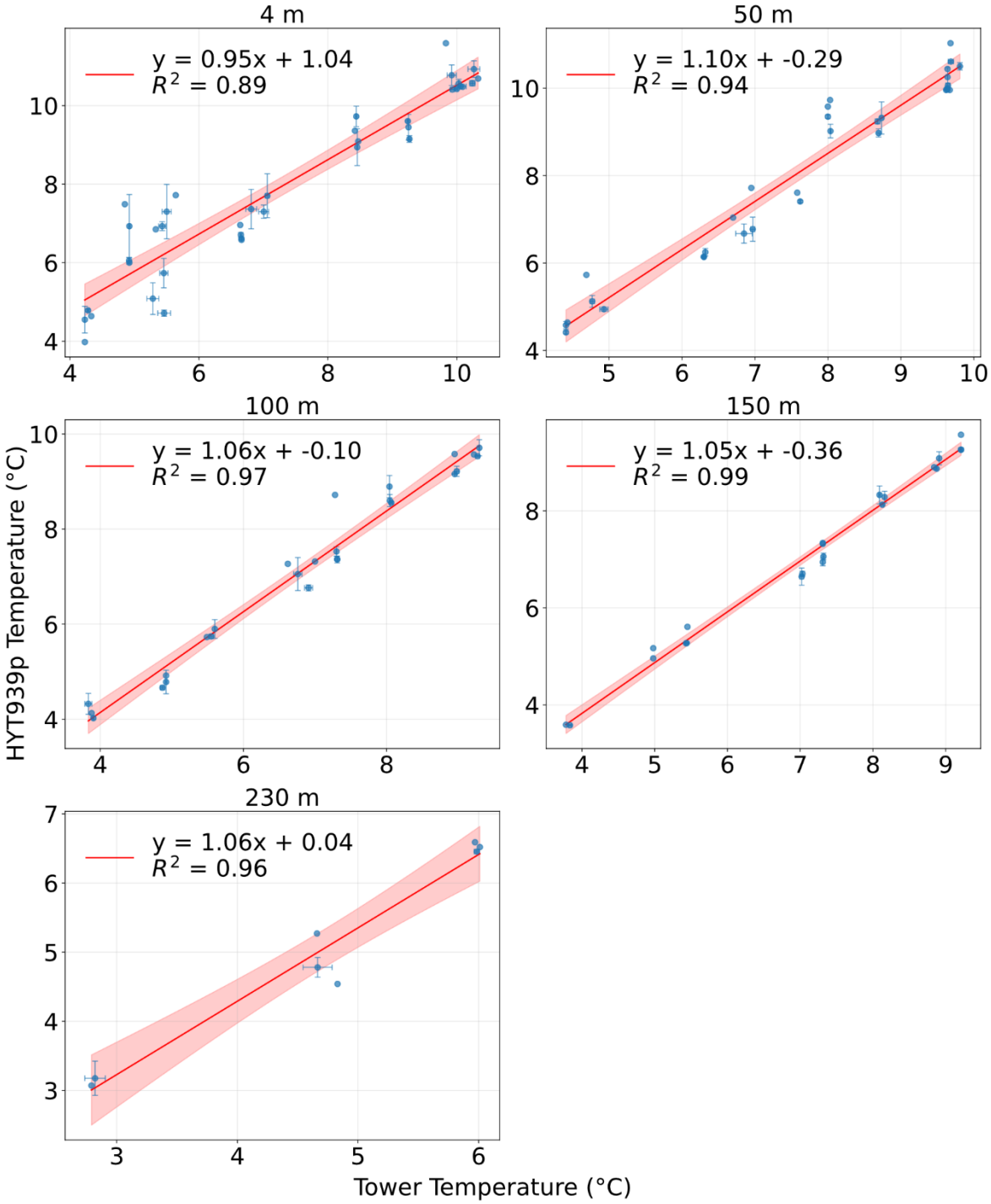

Figure S6. Correlation plot between temperature measurements obtained from the Arduino HYT939p sensor placed on the drone with AE51 and from the sensors on the tower.

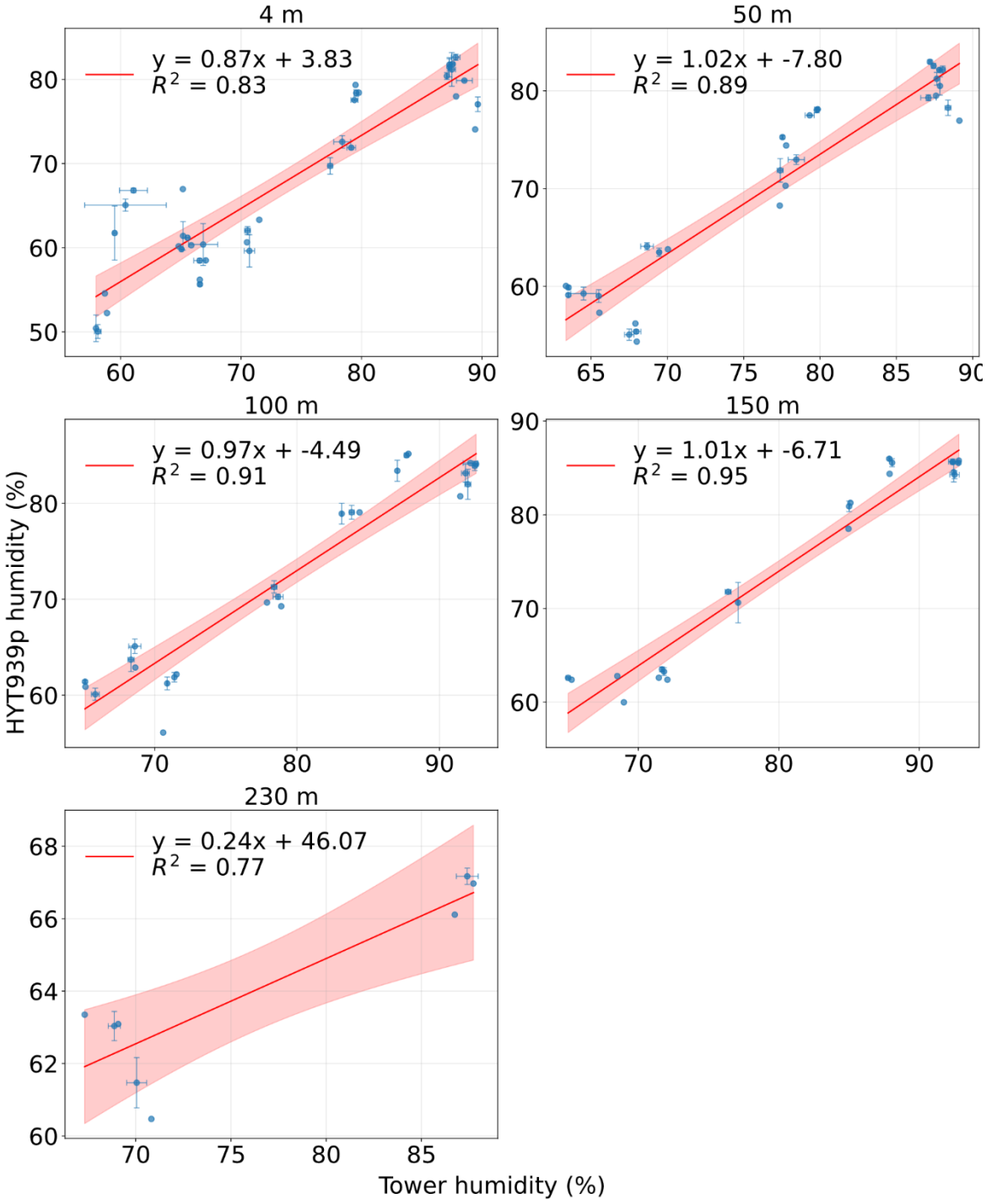

Figure S7. Correlation plot between relative humidity measurements obtained from the Arduino HYT939p sensor placed on the drone with AE51 and from the sensors on the tower.

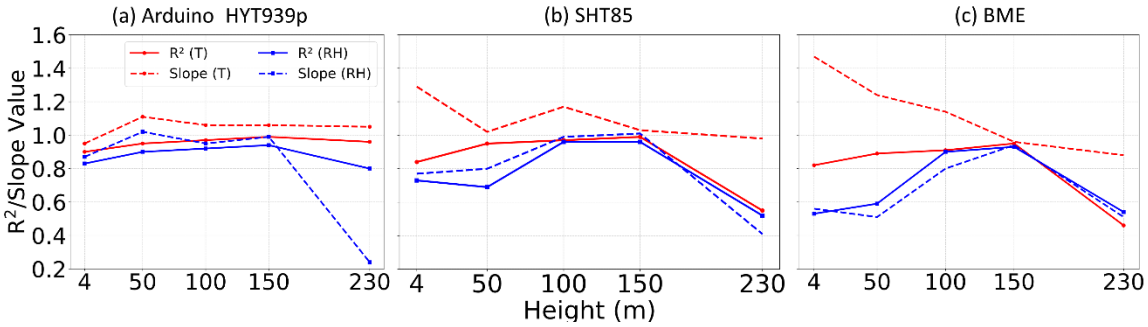

Figure S8. Coefficients of determination (R^2, solid) and regression slopes (dashed) between UAV and tower measurements of T (red) and RH (blue) for (a) Arduino HYT939P, (b) SHT85, and (c) BME sensors at various heights.

Table S1: Table SXX. Geometry and operating parameters of inlets used for Particle Loss Calculator simulations, inclination (0° = horizontal, 90° = vertical), and curvature angle (90° = angle bend). NA = not applicable.

Device (particle size)	Flow Rate	Inlet	Tube Length (m)	Diameter A (mm)	Diameter B (mm)	Angle of Inclination	Angle of curvature
AE51 with dryer (0.01 – 2.5 µm)	0.15 (L/min)	Vertical	0.045	3.5	3.5	90	0
			0.135	6.6	6.6	90	0
			0.01	3	3	90	0
			0.06	3	3	0	90
			0.03	3	3	0	90
AE51 without dryer (0.01 – 2.5 µm)	0.15 (L/min)	Vertical	0.27	3	3	90	0
			0.03	3	3	0	90
OPC (0.35 – 40 µm)	0.28 (L/min)	Horizontal	0	6	6	NA	NA
OPS (0.3 – 10 µm)	1 (L/min)	Vertical	0	6.35	6.35	NA	NA

Table S2: Changes in concentrations for different devices and inlets (OPC, OPS, AE51) at various wind speeds and particle sizes (PM_1, $PM_{2.5}$, and PM_{10}). ↑ represents overestimation and ↓ represents underestimation

Device/Inlet type/Sampling	**Loss**	**Inlet Diameter/ Flow Rate**	**Particle size range**	**WS (m/s)**	**PM1**	**PM2.5**	**PM10**
OPC/Horizontal Inlet/Horizontal Sampling	Sampling Loss (%)	6 mm/ 0.28 L/min	0.35 – 10 µm	0 m/s	0 %	0 %	0 %
				2 m/s	10 % ↑	20 % ↑	110 % ↑
				4 m/s	20 % ↑	60 % ↑	390 % ↑
				6 m/s	40 % ↑	125 % ↑	750 % ↑
OPS/Vertical Inlet/Downward Sampling	Sampling Loss (%)	6.35 mm/ 1 L/min	0.3 – 10 µm	0 m/s	0 %	0 %	14 % ↓
				2 m/s	0 %	0 %	94 % ↓
				4 m/s	4 % ↑	6 % ↑	100 % ↓
				6 m/s	10 % ↑	12 % ↑	100 % ↓
AE51/Vertical Inlet/Downward Sampling	Whole Inlet (Particle Loss (%))	6.35 mm/ 0.15 L/min	0.01 – 2.5 µm	0 m/s	0 %	2 % ↓	NA
				2 m/s	2.5 % ↑	0 %	NA
				4 m/s	10 % ↑	4 % ↑	NA
				6 m/s	22.5 % ↑	3 % ↑	NA

AE51 Dryer/Vertical Inlet/Downward Sampling	Whole Inlet (Particle Loss (%))	6.35 mm/ 0.15 L/min	0.01 – 2.5 µm	0 m/s	0 %	0.6 %	NA
				2 m/s	5 % ↑	9 % ↑	NA
				4 m/s	18 % ↑	30 % ↑	NA
				6 m/s	35 % ↑	50 % ↑	NA

Table S3: Root-mean-square error (RMSE) between UAV and tower measurements of temperature and relative humidity at different heights for Arduino HYT939P, SHT85, and BME sensors.

Height (m)	Arduino HYT939p		SHT85		BME	
	T (°C)	RH (%)	T (°C)	RH (%)	T (°C)	RH (%)
4	0.93	7.19	1.99	7.64	2.50	9.32
50	0.64	6.99	0.68	7.18	1.18	7.76
100	0.44	7.36	0.60	5.49	1.10	7.59
150	0.22	6.41	0.26	4.51	0.43	5.55
230	0.43	13.66	2.41	17.11	2.71	17.23

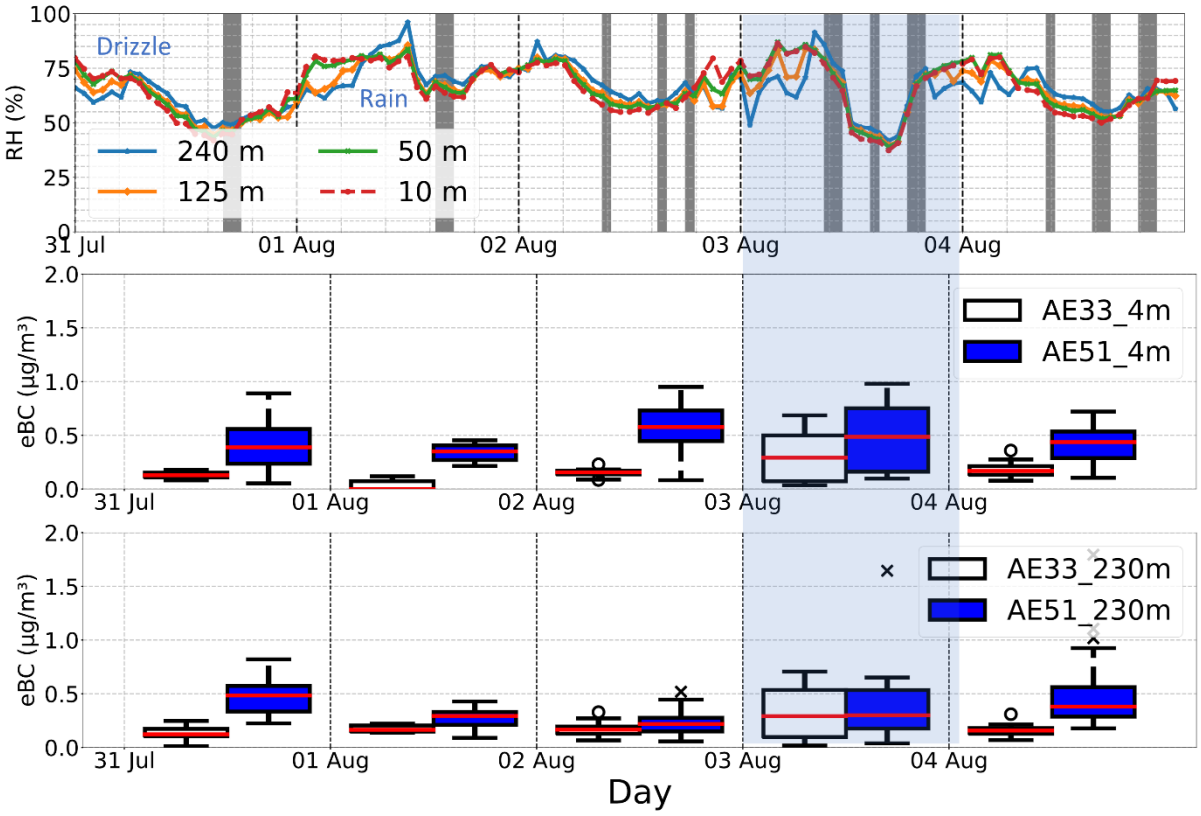

Figure S9. Variation of RH (top) from different heights of tower, eBC concentration from AE51 on drone and AE33 at 4m (middle) and 230m (bottom) during summer measurements at NAOK from July 31 to August 4, 2023. Shaded areas denote drone-AE51 measurement periods

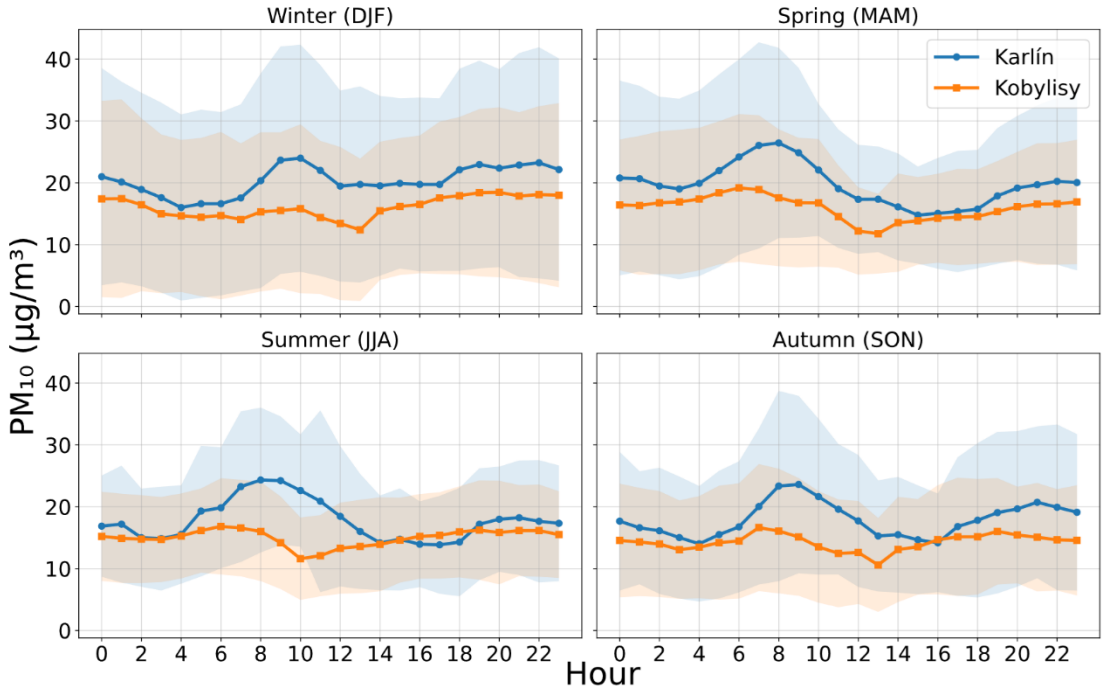

Figure S10: Seasonal diurnal variation of PM_{10} at CHMI stations Karlín (traffic site) and Kobylisy (urban background) during 2023.

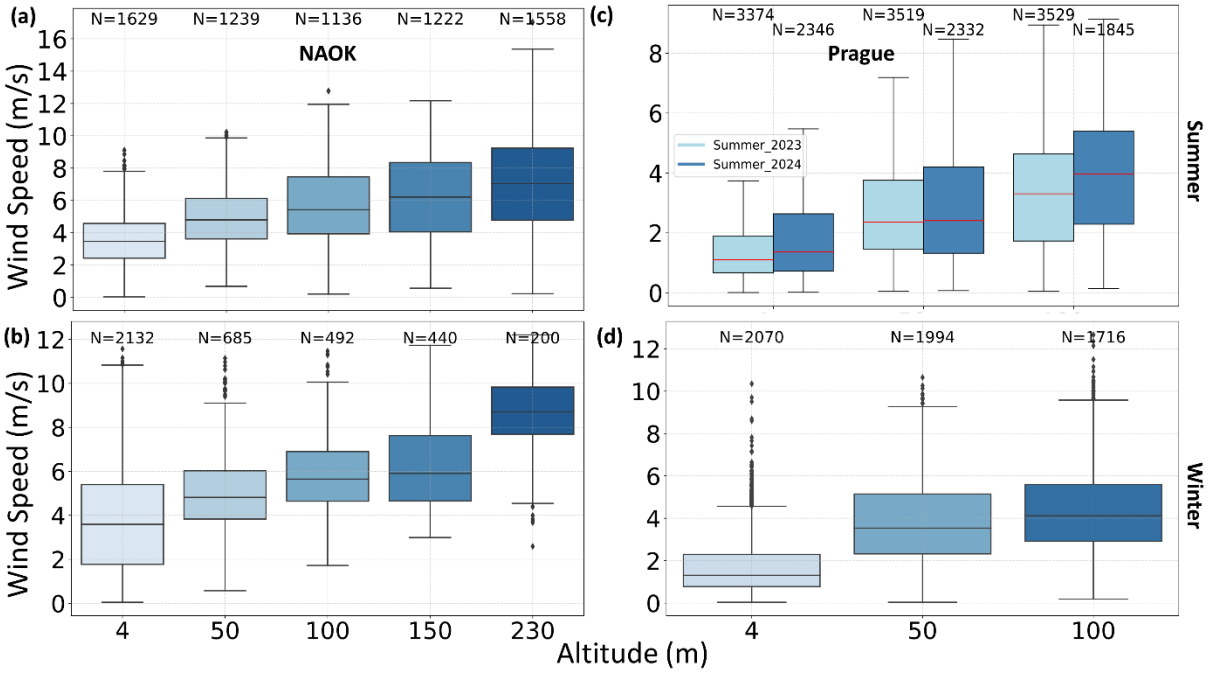

Figure S11. Wind speed at different altitudes from drone at NAOK during (a) summer 2023, (b) winter 2023 and at Prague in (c) summer 2023 and 2024, and (d) winter 2023.

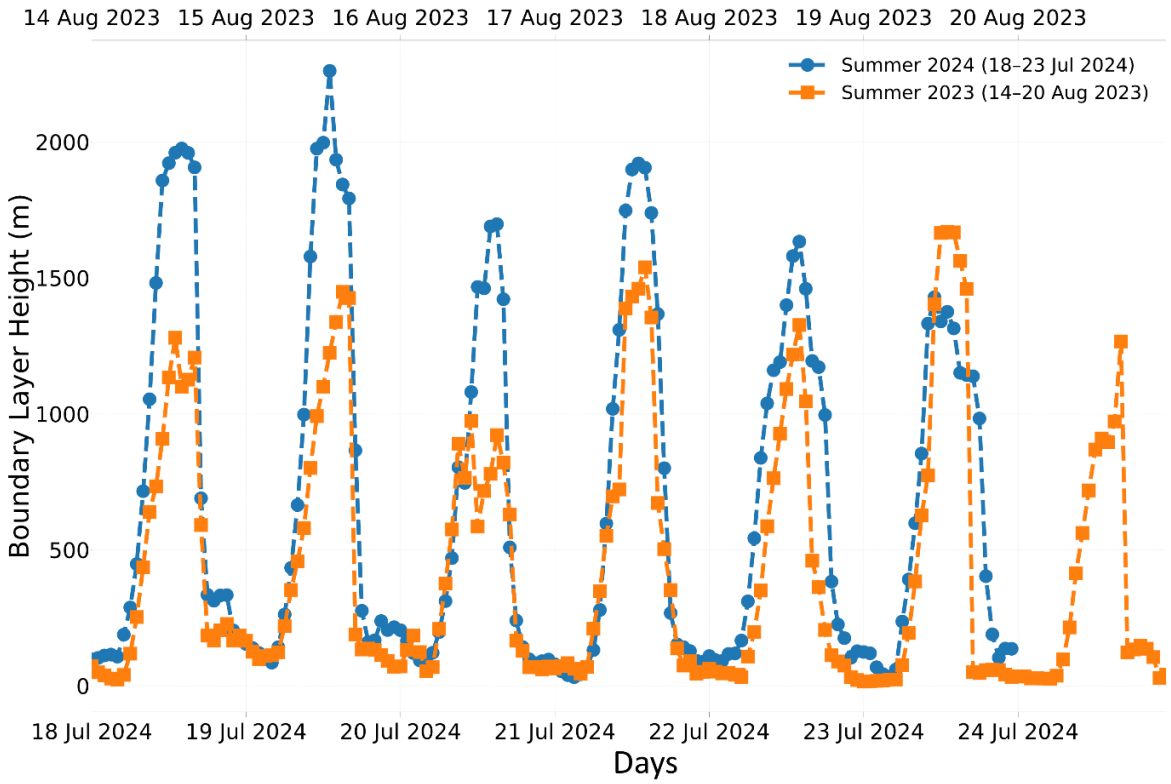

Figure S12: Daily evolution of the boundary-layer height (BLH) during the summer campaigns in 2023 and 2024.

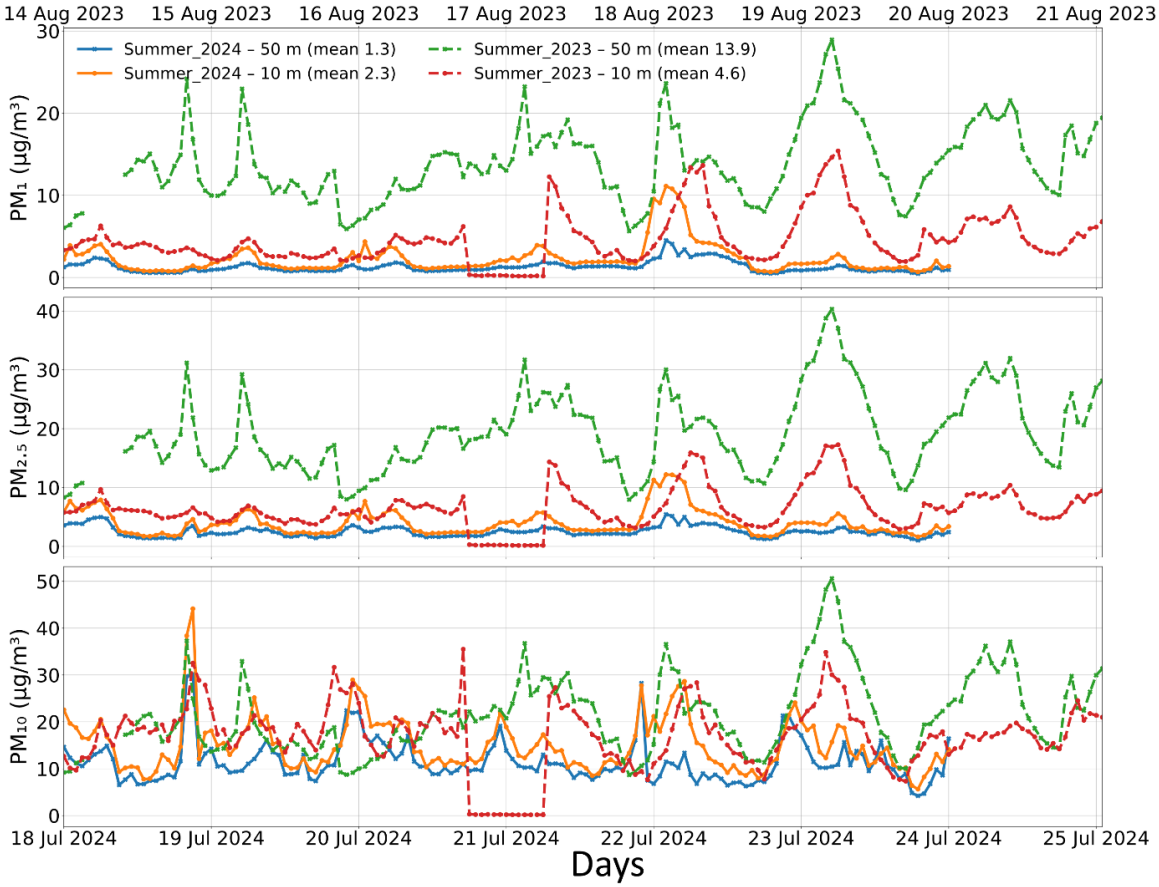

Figure S13: Time series of PM_1, $PM_{2.5}$, and PM_{10} concentrations measured at 10 m and 50 m at the Prague site during summer 2023 (dashed lines) and summer 2024 (solid lines).

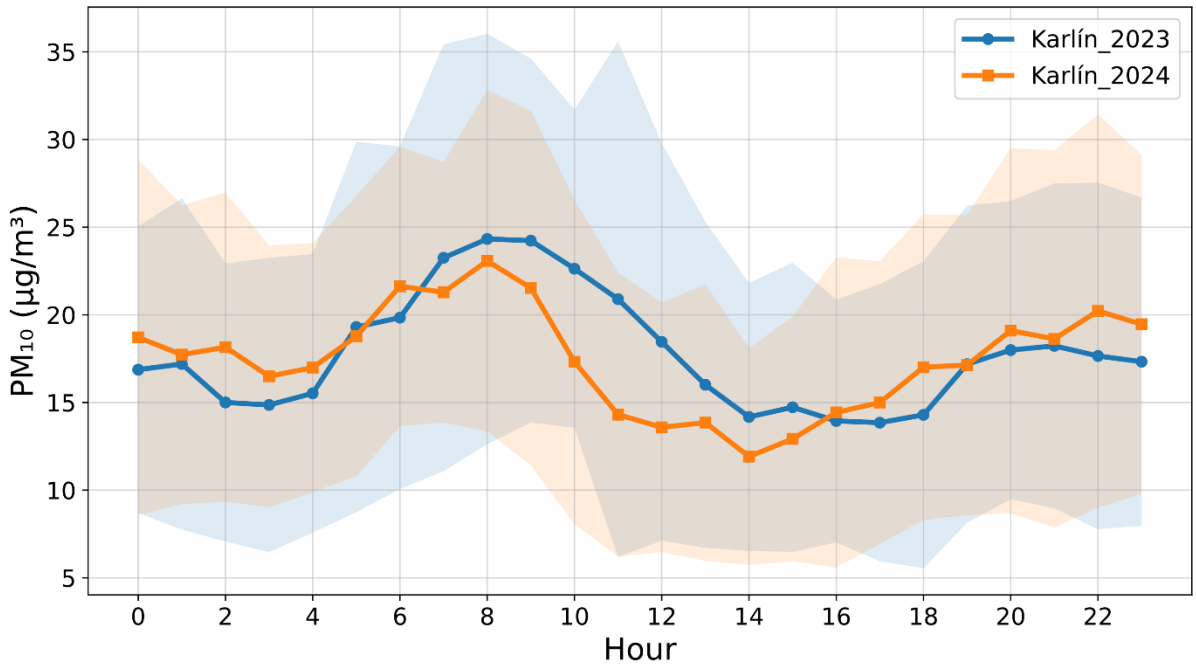

Figure S14: Diurnal variation of PM_{10} at CHMI station Karlín (traffic site) during summer 2023 and 2024.

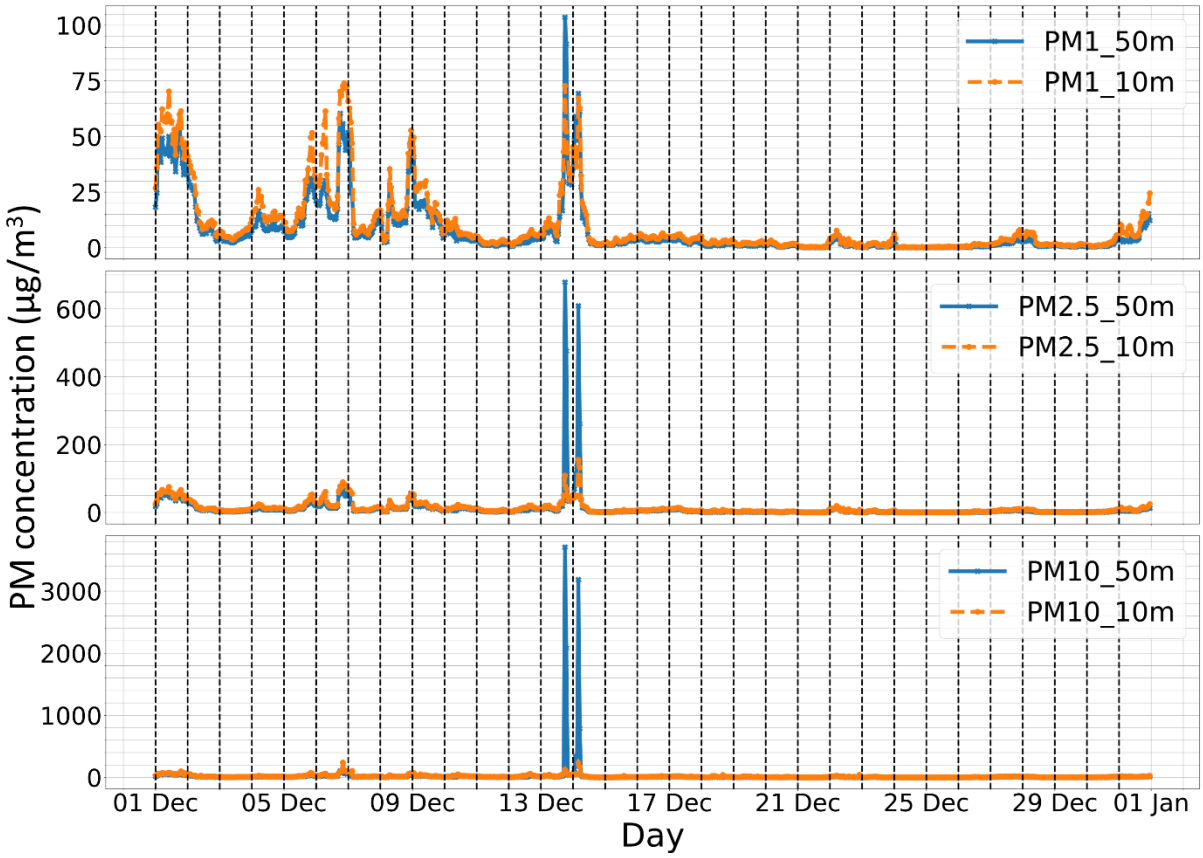

Figure S15 Variation of PM_1 (top), $PM_{2.5}$ (middle), and PM_{10} (bottom) at 10m (orange) and 50m (blue) at Prague during December 2023.

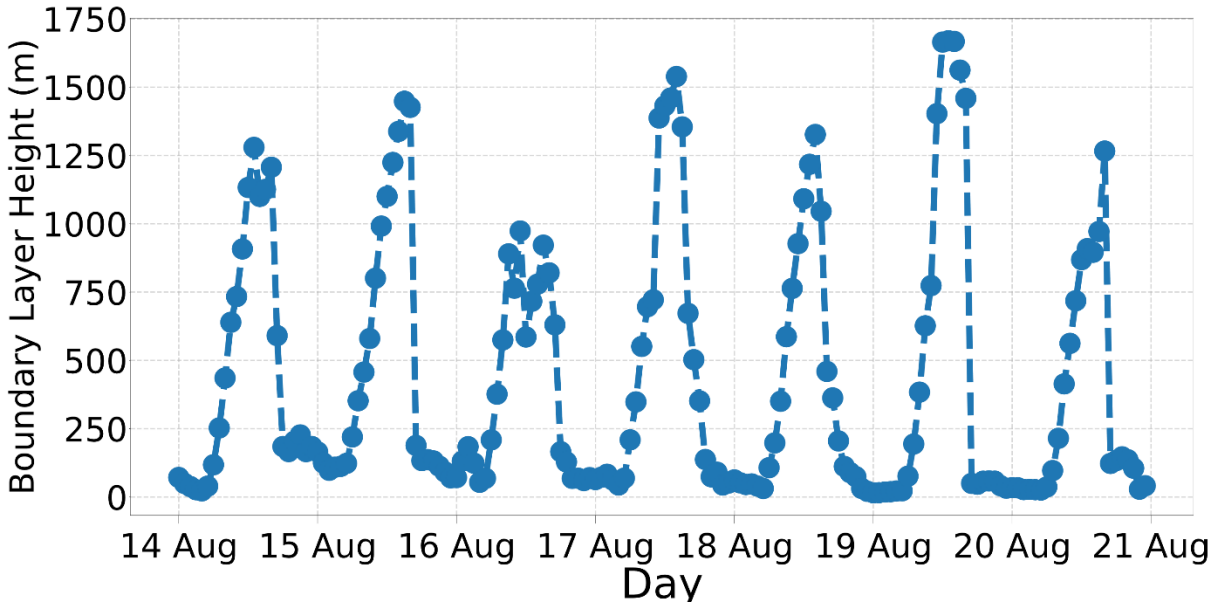

Figure S16. Variation of boundary layer height during winter campaign at Prague. The red circled area indicates the high pollution event.

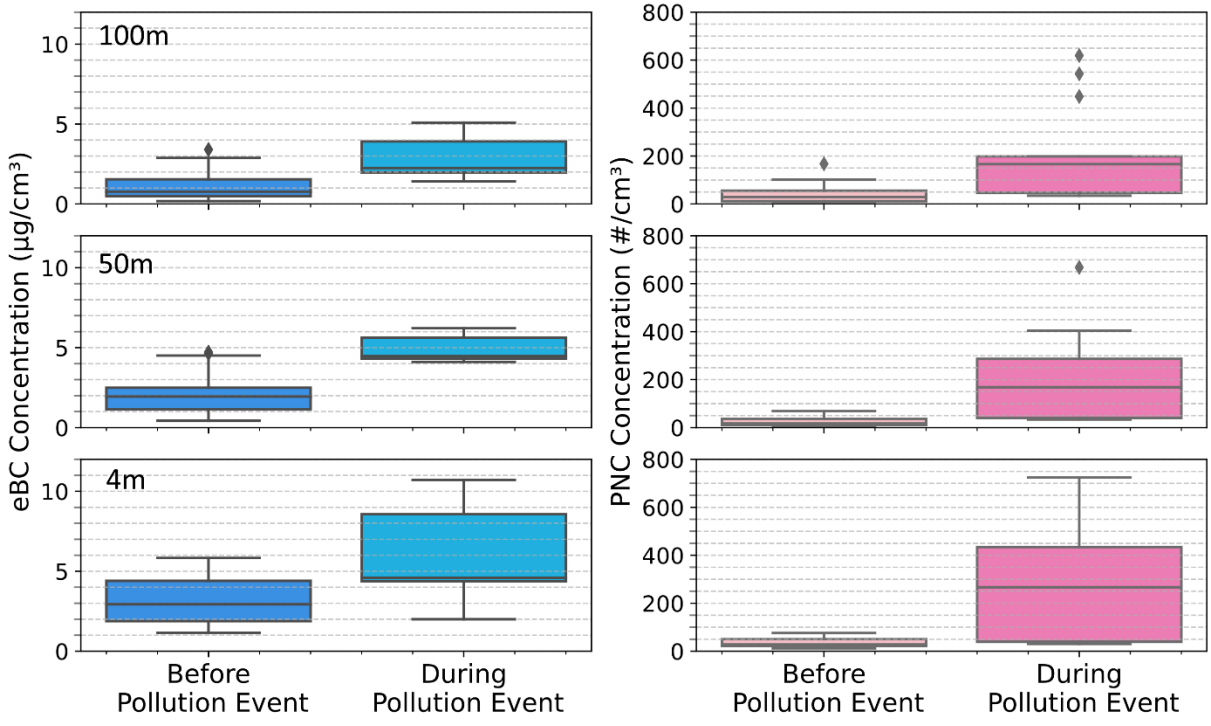

Figure S17. Boxplots of eBC mass concentration from AE51 and PNC from OPC on the drone before and during the high pollution event in Prague at 4 m, 50 m, and 100 m.

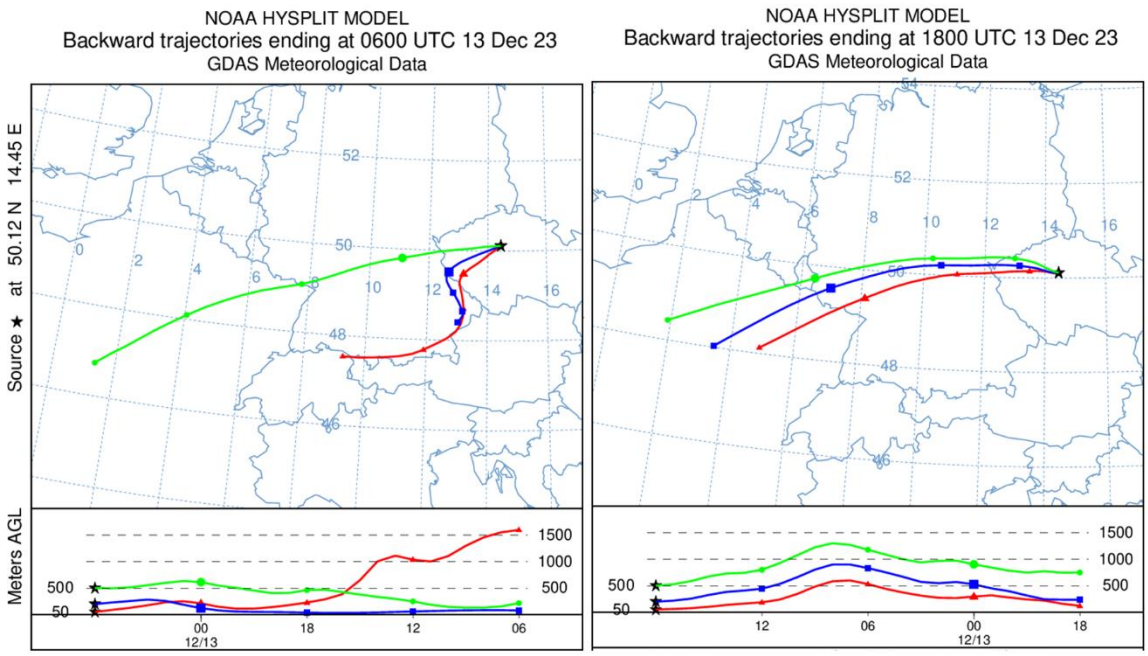

88

89 **Figure S18. HYSPLIT back trajectories at various heights during high pollution episode (left) and before the episode**
90 **(right).**

91

92

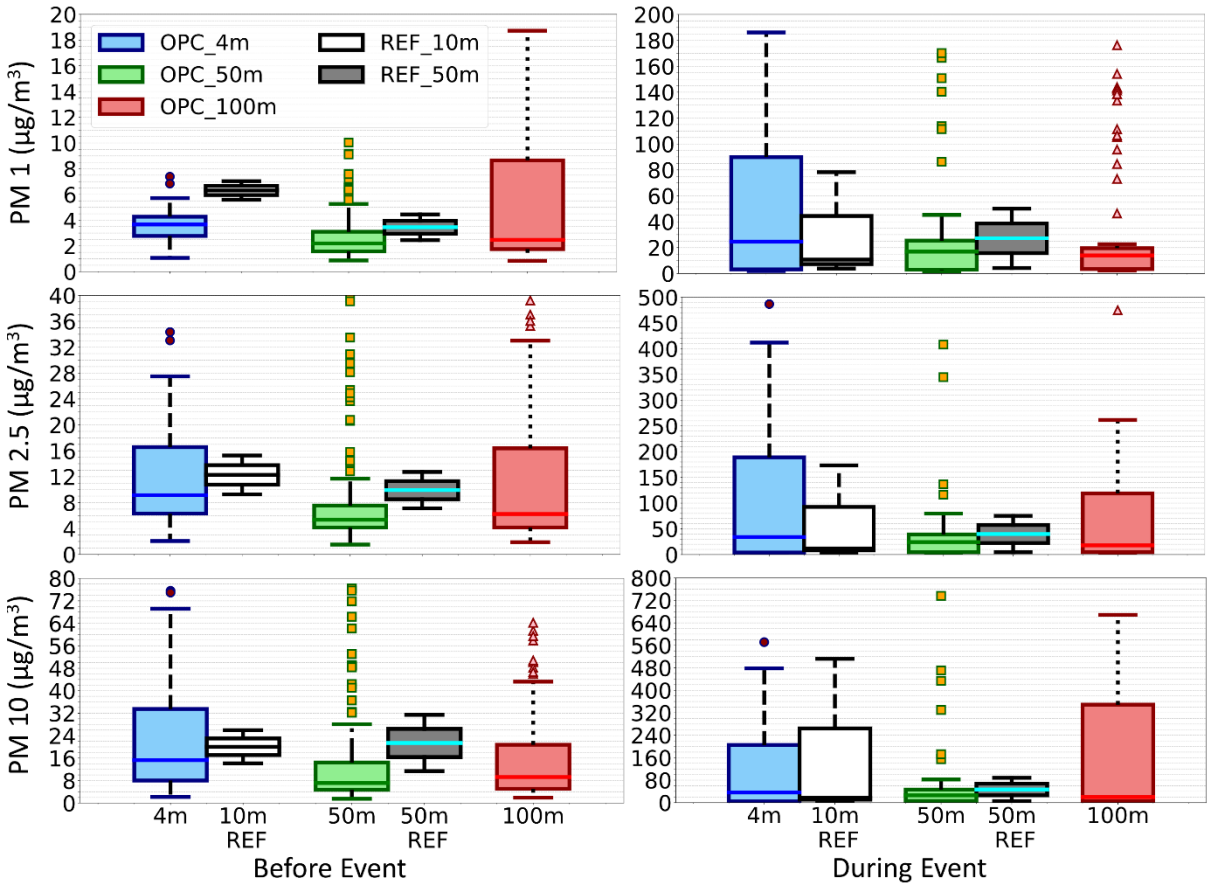

93

94 **Figure S19. Boxplots comparing PM_1, $PM_{2.5}$, and PM_{10} concentrations measured by the OPC on the drone and**
95 **reference devices at 4 m, 50 m, and 100 m above ground level in Prague. Note different y-axis between left and right**
96 **part of the plot.**

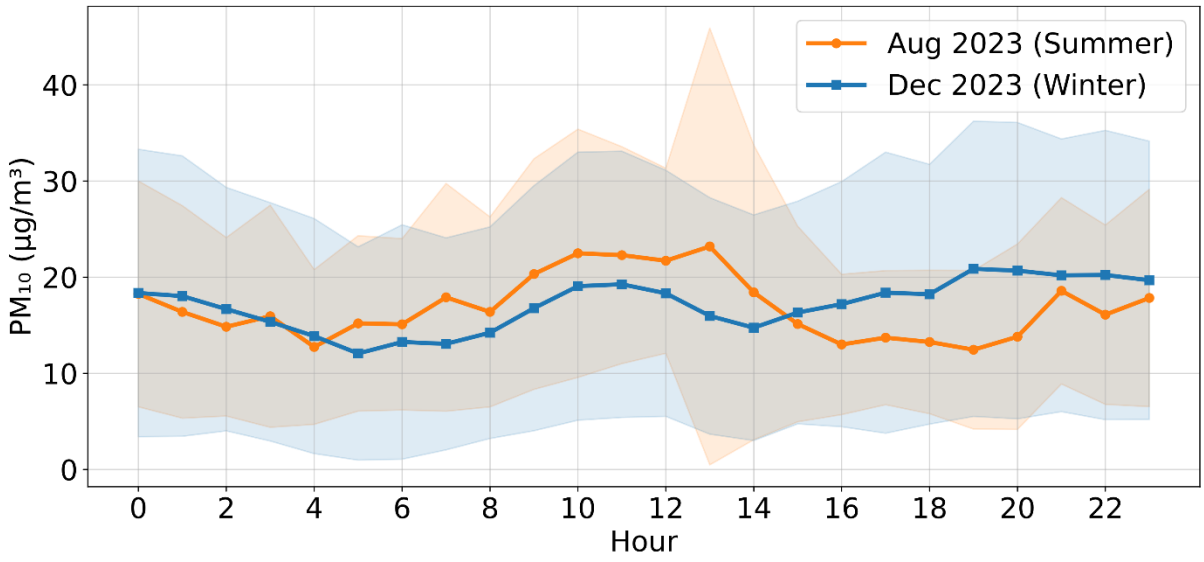

Figure S20: Diurnal variation of mean PM_{10} concentration at the Karlín station during August 2023 (summer) and December 2023 (winter). Shaded areas represent the standard deviation.

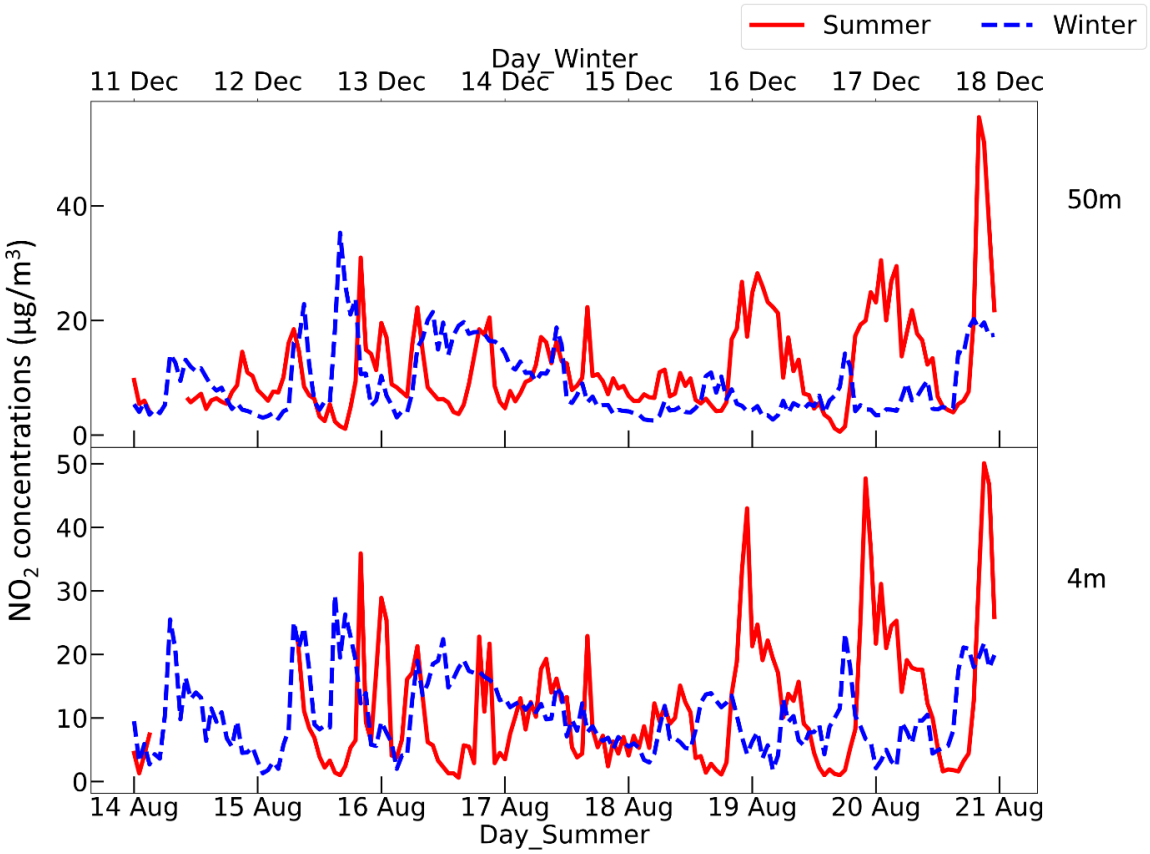

Figure S21. Variation of NO_2 concentrations during summer (red) and winter (blue) campaigns at 4m and 50m at Prague.

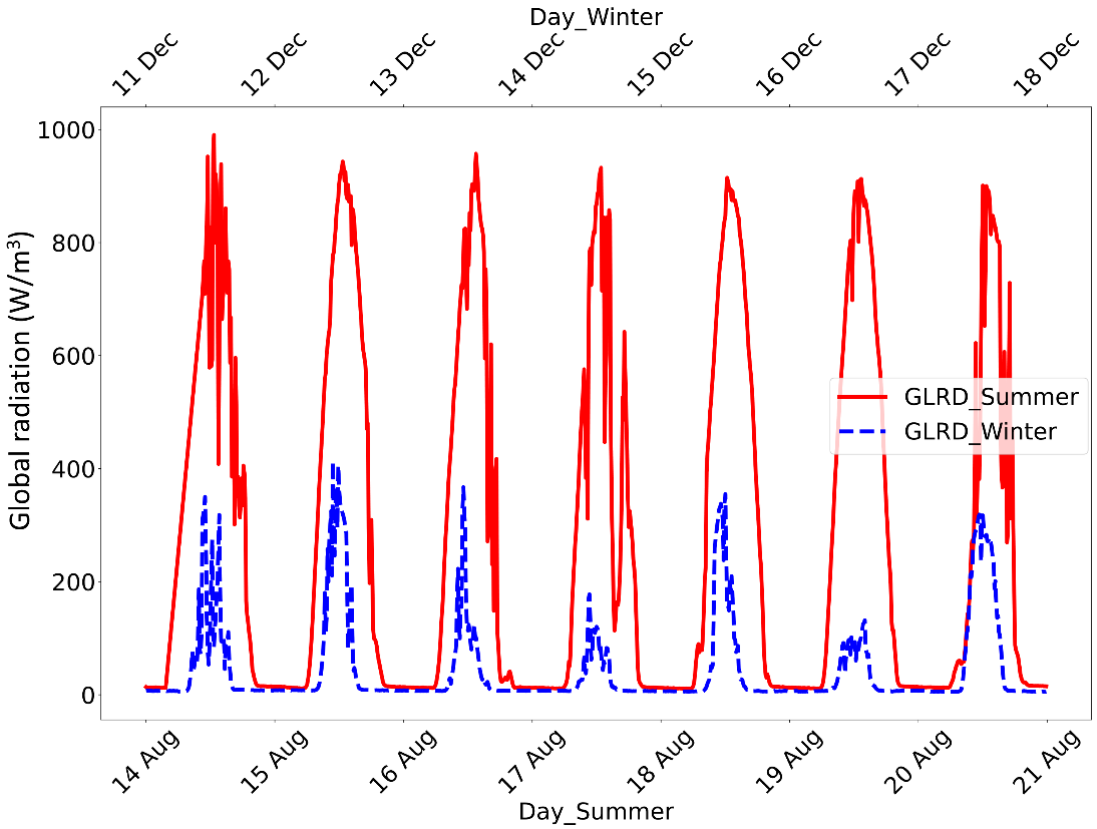

104

105 **Figure S22. Variation of global radiation during summer (red) and winter (blue) campaign at Prague.**

106